J Solid State Electrochem (2005) 9: 284–289
DOI 10.1007/s10008-004-0599-5

ORIGINAL PAPER

W. Huang · Z. L. Li · Y. D. Peng · S. Chen
J. F. Zheng · Z. J. Niu

Oscillatory electrocatalytic oxidation of methanol on an $Ni(OH)_2$ film electrode

Received: 26 August 2004 / Revised: 7 September 2004 / Accepted: 9 September 2004 / Published online: 21 January 2005

Abstract A film of $Ni(OH)_2$ deposited cathodically on a roughened nickel substrate consists of even nanoparticles, which were characterized by atomic-force microscopy (AFM). The mechanism of potential oscillations in the electrocatalytic oxidation of methanol on this film electrode in alkaline medium was studied in situ by means of Raman spectroscopy in combination with electrochemical measurements. The redox change of the nickel hydroxide film, the concentration distribution of methanol in the diffusion layer, and the oxidation products of methanol were characterized in situ by time-resolved, spatial-resolved, and potential-dependent Raman spectroscopy, respectively. Electrochemical reactions, i.e. methanol oxidation and periodic oxygen evolution, coupling with alternately predominant diffusion and convection mass transfer of methanol, account for the potential oscillations that occur during oxidation of methanol above its limiting diffusion current. This mechanism is totally different from that of methanol oxidation on platinum electrodes, for which surface steps, i.e. formation and removal of CO_{ad}, are essential.

Keywords Nano-structured nickel hydroxide film · In-situ Raman spectroscopy · Potential oscillations · Methanol · Mechanism

This work is dedicated to Professor Gyorgy Horanyi on the occasion of his 70th birthday in recognition of his numerous contributions to field of electrochemical oscillations and electrocatalysis at Ni-hydroxide electrodes.

W. Huang · Z. L. Li (✉) · J. F. Zheng · Z. J. Niu
Zhejiang Key Laboratory for Reactive Chemistry on Solid Surfaces, Institute of Physical Chemistry, Zhejiang Normal University, Jinhua, 321004, China
E-mail: lizelin@zjnu.cn
Tel.: +86-579-2283897
Fax: +86-579-2282595

Z. L. Li · Y. D. Peng · S. Chen
Department of Chemistry, Hunan Normal University, Changsha, 410081, China

Introduction

Since the series of reports by Mueller and co-workers in 1920s [1–3], electrochemical oscillations in the electrocatalytic oxidation of methanol, formic acid, and formaldehyde on Pt and Pt-based metals have attracted great interest [4], owing to their fundamental importance as model systems [5]. It is generally accepted that the electrocatalytic oxidation of methanol, like formic acid and formaldehyde, into CO_2 on platinum is via a dual-path mechanism that was elucidated by a variety of in-situ techniques [6–12]. The formation and removal of CO_{ad} are the main reasons for the oscillations on the noble metal electrode.

Some non-noble metal materials can also have electrocatalytic activity toward the oxidation of small organic molecules. Among these, nickel is the most widely studied. For example, electro-syntheses of some carboxylic acids and ketones on nickel hydroxide have been well documented [13, 14], nickel-based electrodes have been used to detect carbohydrates, amines and amino acids [15–20], and electrocatalytic oxidation of alcohols, amines, etc., has been performed on nickel hydroxide, nickel-based complexes or alloys [21–35]. An indirect electron-transfer process occurs through the redox pair $Ni(OH)_2$/NiOOH in the electrocatalytic oxidation of small organic molecules [21].

Recently, we discovered potential oscillations during methanol electrocatalytic oxidation on a nano-structured nickel hydroxide film (NNHF) electrode [36]. Owing to the high electrocatalytic activity of the NNHF electrode, alternatively dominant diffusion and convection mass transfer plays the key role in the oscillations, instead of the formation and removal of CO_{ad} as on the Pt electrode. In this paper, we report detailed studies of the new oscillatory mechanism for methanol electro-oxidation on the NNHF electrode by means of surface morphology, in-situ spatiotemporal-resolved Raman spectroscopy, and electrochemical measurements.

Materials and methods

Raman spectra were obtained with a Reinshaw RM1000 microscopical confocal Raman spectrometer (UK). Unless indicated, the exciting wavelength was 632.8 nm from an air-cooled He–Ne laser with a power ca. 3 mW on the sample. Detailed description of the Raman measurements can be found elsewhere [12, 37]. Electrochemical measurements were carried out with a CHI 660 A Electrochemical Station (CHI Instruments, USA) interfaced with a computer. A nickel disk (1 mm diameter), a platinum wire in a circle, and a saturated mercurous sulfate electrode (SMSE) with a Luggin capillary were employed as the working, counter, and reference electrodes, respectively. A polycrystalline Pt wire working electrode (1 mm in diameter and 8.5 mm in length) was also used for comparison. All solutions were freshly prepared with triply distilled water and analytical-grade chemicals. The film of $Ni(OH)_2$ was deposited on a nickel disk, roughened by $04^{\#}$ metallographic paper, under cathodic galvanostatic conditions, typically 600 μA cm^{-2} for 1200 s in 0.01 mol dm^{-3} $Ni(NO_3)_2$. The film electrode was pretreated using cyclic voltammetry (CV) in background solution (1 mol dm^{-3} NaOH) until repeatable voltammograms were obtained. The surface structure of the film electrode was analyzed in situ by means of a Leica microscope and ex situ by atomic force microscopy (AFM) (Solver P47H). A semi-contact mode was adopted in the AFM analysis to avoid damaging the film.

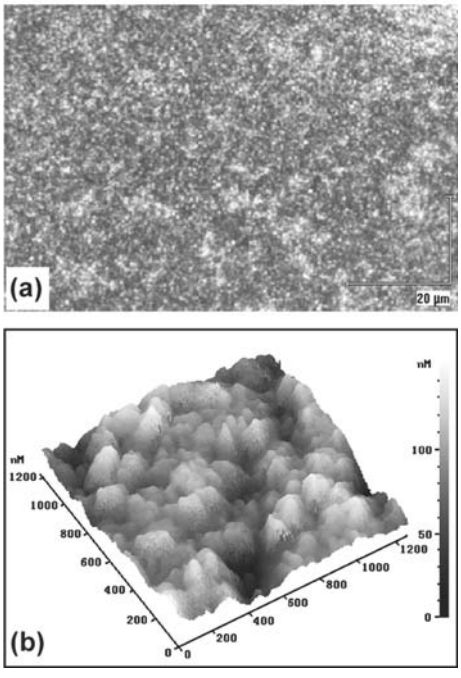

Fig. 1 **a** In situ microphotograph and **b** ex situ AFM image of the nickel hydroxide film (NHF) electrode after potential cycling between −0.6 and 0.2 V in 1 mol dm^{-3} NaOH solution

Results and discussion

Nano-structure of the nickel hydroxide film electrode

The surface morphology of the film electrode pretreated in the background solution by CV was examined both in situ by use of a Leica microscope (×500) and ex situ by AFM. As shown in Fig. 1a in large scale obtained with the Leica microscope, the surface is thickly dotted with even particles. The average diameter of the particles is not beyond 100 nm, estimated from the AFM image (Fig. 1b). The porous film of $Ni(OH)_2$ prepared in this way has a high surface area and better electrocatalytic activity for methanol oxidation.

Electrochemical behavior

Cyclic voltammograms

The solid lines in Fig. 2 show the CVs of methanol oxidation on the mechanically roughened nickel substrate (a), on the NNHF electrode (b), and on polycrystalline platinum (c). On account of the better electrocatalytic activity of the NNHF, the anodic peak current on this electrode (the thicker solid line in Fig. 2b) decuples that on the roughened nickel electrode

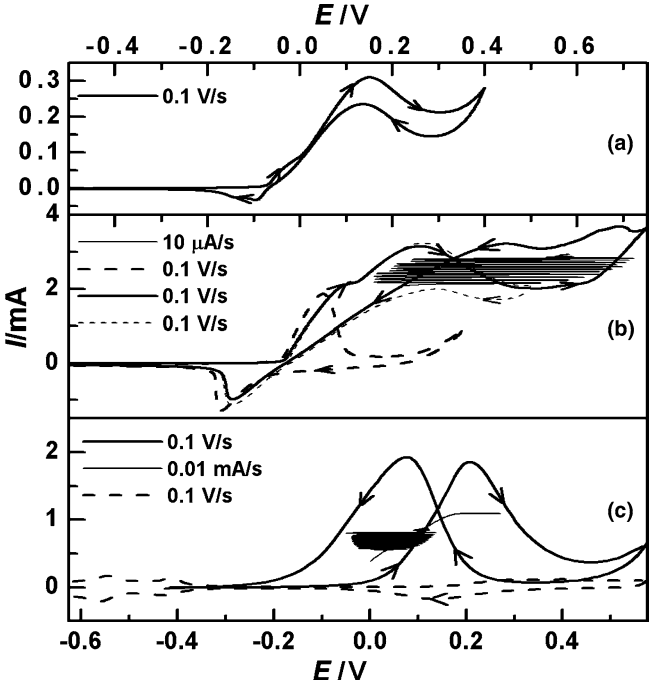

Fig. 2 Voltammograms at 100 mV s^{-1} on **a** the roughened nickel electrode, **b** the NHF electrode in a solution of 1 mol dm^{-3} NaOH with (*solid line* and *thinner dashed line*) or without (*dashed line*) 1 mol dm^{-3} CH_3OH, and **c** platinum wire electrode in a solution of 1 mol dm^{-3} H_2SO_4 with (*solid line*) or without (*dashed line*) 1 mol dm^{-3} CH_3OH. The *thinner solid lines* in **b** and **c** represent current scan curves at 10 μA s^{-1} and 0.01 mA s^{-1}, respectively

(Fig. 2a) for methanol oxidation. So we can deduce that the contribution from the substrate is small during decomposition of methanol on the NNHF anode. There are two ascending branches in the CV curve for the NNHF electrode (the thicker solid line in Fig. 2b) during the forward potential scan, which represent two different reaction processes in the electrocatalytic oxidation of CH_3OH. Note that oxygen evolution occurs only in the second ascending branch. Bistable states (methanol oxidation with and without oxygen evolution at higher and lower potentials, respectively) possibly occur in a range of currents where one current (as a level line) connects two different points in the two ascending branches. Between them there is a descending branch, and the point in this curve represents an unstable state. This descending branch comes from the diffusion-limited depletion of the methanol surface concentration. A limiting current plateau appears instead with a slower potential scan (Fig. 2a in [36]), confirming that diffusion mass transfer is the rate-determining step in methanol oxidation on the NNHF electrode. The shoulder peak at 0.1 V is due to the conversion of $Ni(OH)_2$ into NiOOH, which accompanies a fast color transition from light green to black. This is a typical electrochromic process [38]. The reductive current for the NiOOH becomes smaller while methanol is present (Fig. 2b), which indicates that some NiOOH that is produced during the forward potential scan is transferred into the $Ni(OH)_2$ again by oxidizing methanol. A similar situation occurs on the platinum electrode, i.e. no or less reductive current appears for the backward scan (the thicker solid line in Fig. 2c) in the presence of methanol.

Noticeably, the solid lines in the CVs for the electrocatalytic oxidation of methanol on both the NNHF (Fig. 2b) and Pt (Fig. 2c) electrodes show crossing cycles, where the current for the backward potential scan is larger than that for the forward scan. The crossing cycle means there are a pair of positive and negative feedbacks overlapping within the bistable range. This is a common characteristic for electrochemical oscillatory systems [39, 40]. With the crossing cycle one can easily judge whether oscillations and what kinds of oscillations could occur [39, 40]. According to this criterion, potential oscillations could be expected to occur in the two electrochemical systems. Although potential oscillations in the electro-oxidation of methanol on Pt electrodes have been widely studied [5, 36, 41], no such reports have appeared in the literature on nickel or nickel hydroxide film electrodes, except for our recent preliminary results [36].

Remarkable differences between the locations of the two crossing cycles are apparent from comparison of Figs. 2c and 2b; these are indicative of different electrocatalytic and oscillatory mechanisms for the methanol oxidation on the two electrodes.

We can see in Fig. 2c that the crossing loop on Pt lies in the range of about −0.2–0.1 V, i.e. in the ascending branch of the first oxidation peak. Surface ad/desorptive processes of CO are the main reason for this crossing cycle. At lower potentials, surface bonded CO_{ad} formed by dissociation of methanol occupies the most active sites of the electrode surface. The poisonous intermediate (CO_{ad}) suppresses hydrogen ad/desorption and methanol oxidation over a wider potential range. So the methanol oxidation current in the double-layer region is smaller during the forward potential scan. The oxygen species involved in the reaction in the double layer region arise mainly from the surface-adsorbed water molecules [5, 41]. At higher potentials, CO_{ad} can be effectively removed by reaction with OH_{ad} that is produced in the oxygen-adsorption region. The removal of CO_{ad} in this way explains not only the disappearance of the reduction peak of oxygen species that occurs in the absence of methanol, but also the larger oxidation current in the double-layer region during the backward potential scan. The formation and removal of CO_{ad} constitute the main positive and negative feedback steps. Bistable states possibly occur in the crossing loop (Fig. 2c) that consists of the first ascending branch and the last descending branch for forward and backward scanning, respectively. These two branches represent methanol oxidation with more and less CO_{ad} presence, respectively. The consistency of potential regions for the oscillation (the thinner solid line in Fig. 2c) and for the crossing loop (the thicker solid line in Fig. 2c) confirms the validity of these explanations and the CV criterion [39, 40]. Such an oscillator can be classified as the coupling of electrochemical reactions with ad/desorption from the point of view of electrode processes [39, 40].

Whereas the crossing loop on the NNHF appears in a higher potential range from 0.3 to 0.7 V, falling in the descending branch of the first oxidation peak (Fig. 2b). Oxygen evolution occurs in the second ascending branch during the forward potential scan. Therefore the larger current in the backward potential scan is exclusively owing to the enhanced convection mass transfer of methanol from oxygen evolution. Note that no crossing loops can be observed when the potential scan is reversed before oxygen evolution (the thinner dashed line in Fig. 2b). Unlike on the Pt electrode, potential oscillations on the NNHF electrode (the thinner solid line in Fig. 2b) belong to a different category, i.e. the coupling of electrochemical reactions with diffusion and convection mass transfer [39, 40]. More detailed discussion of the oscillatory electrocatalytic oxidation of methanol on the NNHF electrode will be given in following sections.

Galvanostatic potential oscillations

Some typical waveforms in the range of currents in which potential oscillations occur are shown in Fig. 3; these were obtained by constant-current control at 1.8 (a), 2.2 (b), and 2.8 mA (c), respectively. Upon increasing the applied current the oscillatory period gets shorter while the amplitude gets larger. These facts are understandable because (1) the consumption of surface methanol speeds up, which increases the oscillatory

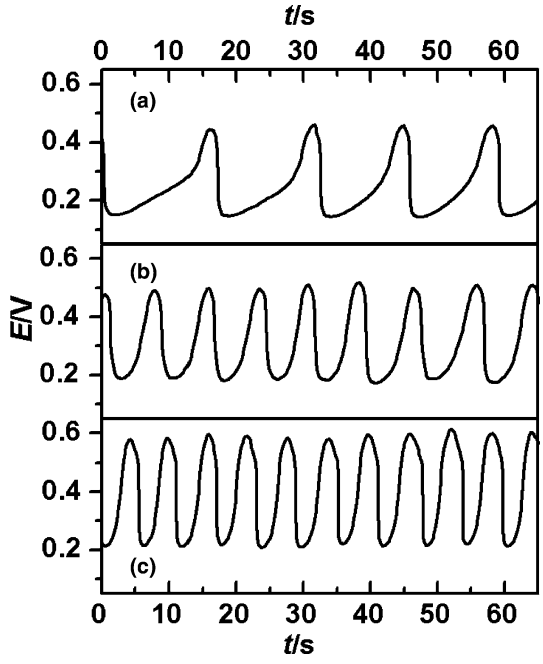

Fig. 3 Time series of potential oscillations for methanol oxidation on the NNHF electrode by constant-current control at **a** 1.8 mA, **b** 2.2 mA, and **c** 2.8 mA

frequency, and (2) the potential rises for oxygen evolution along the I/E curve (the thicker solid line in Fig. 2b), which enlarges the oscillatory amplitude.

In-situ Raman spectroscopy

In-situ Raman spectroscopy can provide us with much mechanistic information at a molecular level. The change of the surface nickel species for the film electrode, the distribution of methanol concentration in the diffusion layer, and the soluble oxidation products of methanol, have all been detected by use of this in-situ technique.

Temporal-resolved Raman spectroscopy

Time-solved Raman spectra were acquired during the open-circuit time after setting the potential at 0.5 V for 10 s. The bands at 476 and 560 cm^{-1} (Fig. 4) are assigned to the Ni-O vibration for NiOOH [42], which is the oxidation product of $Ni(OH)_2$. The intensity of the 476/560 cm^{-1} doublet gradually declined and finally turned disappeared within 300 s of opening the circuit. Meanwhile, the dark color of the electrode surface gradually faded away and a light green color appeared instead during the measurement. These facts indicate that the surface NiOOH was converted into $Ni(OH)_2$ again. Another experiment was also performed under the same conditions but with the background solution only. As a result, both the Raman intensity and the dark color of the electrode surface remained unchanged. Therefore, it can be easily concluded that (1) the electrocatalytic oxidation of methanol is through the redox pair $Ni(OH)_2$/NiOOH, and (2) the rate of transition from $Ni(OH)_2$ to NiOOH is faster than that of reaction between NiOOH and methanol, because the NiOOH produced in 10 s was consumed in 300 s.

Spatial-resolved Raman spectroscopy

The concentration distribution of methanol in the diffusion layer was measured directly by changing the distance between the laser focus and the working electrode surface. Under constant potential control at 0.2 V the intensity of band 1017 cm^{-1} for methanol [25] increases with distance up to about 240 μm (the dashed line in Fig. 5). It is clearly seen that oxidation of methanol is controlled by mass diffusion in the potential range of the limiting diffusion current plateau [36].

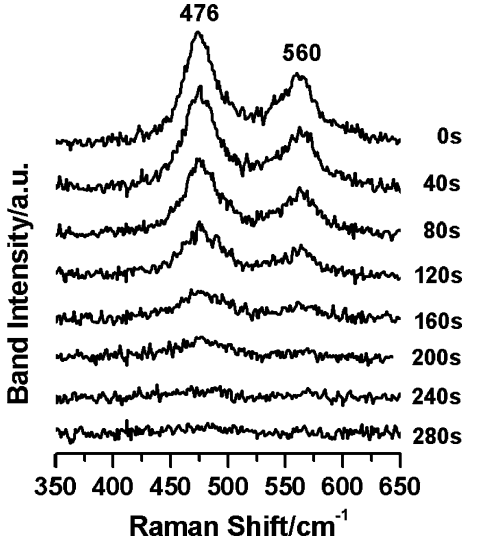

Fig. 4 Raman spectra at the NNHF electrode surface for NiOOH decay during open-circuit time in a solution as used in Fig. 2a. The collection time for recording a single spectrum was 20 s

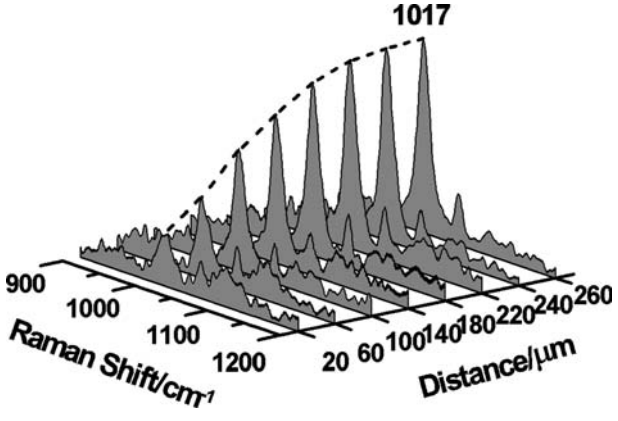

Fig. 5 Spatial-resolved in-situ Raman spectra during methanol electro-oxidation on the NNHF electrode at 0.2 V with a solution as in Fig. 2a. The collection time for recording a single spectrum was 150 s and the dashed line lying at peak 1017 cm^{-1} indicates the methanol concentration profile in the diffusion layer

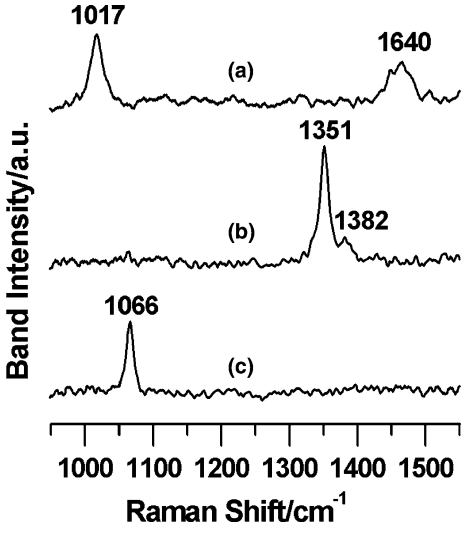

Fig. 6 Raman spectra (Ar^+ laser; 514.5 nm line) for solutions of **a** 1 mol dm^{-3} CH_3OH + 1 mol dm^{-3} NaOH, **b** 0.5 mol dm^{-3} HCOOH + 1 mol dm^{-3} NaOH, and **c** 0.5 mol dm^{-3} Na_2CO_3 + 1 mol dm^{-3} NaOH

Dependence of the Raman spectra on potential

Figure 6 shows the Raman spectra for samples of methanol (a), formate (b) and carbonate (c) in alkaline aqueous solutions. The three groups of vibration bands in Fig. 6, i.e. 1017 with 1460, 1382 with 1351, and 1066 cm^{-1}, are assigned to the ν_s(C-OH) and δ(C-H) from methanol [25, 43], the δ(C-H) or ρ_r(COO) and ν_s(COO) from formate [25, 44, 45], and the ν_s(C-O) from carbonate [25, 46], respectively.

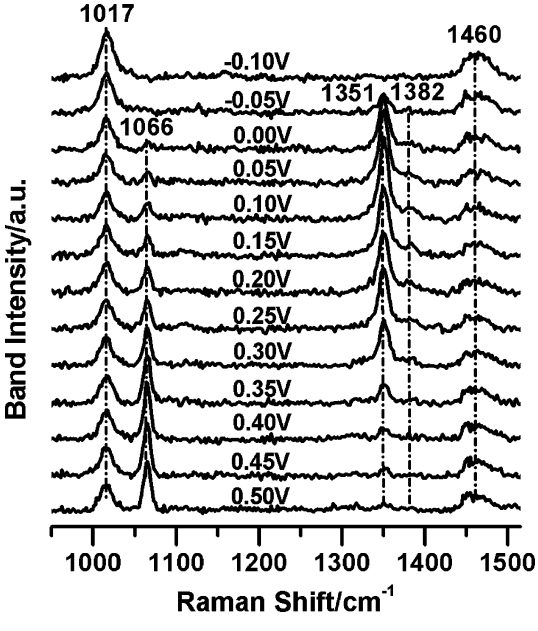

Fig. 7 In-situ Raman spectra (Ar^+ laser; 514.5 nm line) for methanol electro-oxidation on the NNHF electrode at different potentials with the same solution as in Fig. 6a

In-situ Raman spectra for methanol oxidation on the NNHF electrode were measured as a function of electrode potential (Fig. 7). All the in-situ spectra in Fig. 7 were obtained while the laser focus was 100 μm from the NNHF surface. The first spectrum was taken at −0.1 V, a potential where no methanol electro-oxidation occurs. With potential increase from −0.05 to 0.5 V, new features at 1351 and 1382 cm^{-1} for formate appear first, and the peak at 1066 cm^{-1} for carbonate follows. These facts indicate that methanol is oxidized into formate first, and further into carbonate. The band intensity at 1066 cm^{-1} for the final electro-oxidation product increases continuously, owing to the accumulation of carbonate in the diffusion layer, whereas the 1351 and 1382 cm^{-1} doublet first become stronger and then get weaker and weaker, because of the further oxidation of formate into carbonate.

Oscillatory mechanism for the electrocatalytic oxidation of methanol on the NNHF electrode

From analysis of the experimental results given above, a feasible schematic mechanism for the oscillatory electrocatalytic oxidation of methanol on the NNHF has been summarized as in Fig. 8. In the network, trivalent nickel species (NiOOH) are formed via (1). Methanol near the surface is oxidized into formate via (2) and further into carbonate via (3). When the applied current rises above the stationary limiting oxidation current of methanol, the surface concentration of methanol is soon depleted to zero owing to its limited rate of supply by diffusion. Meanwhile, the potential moves positively with decreasing methanol surface concentration, until oxygen evolution takes place via (4) to keep up the applied current, whereas the growth, detachment and movement of the oxygen bubbles cause forced convection mass transfer via (5). The potential thus drops, due to the replenishment of the methanol surface concentration. A new cycle repeats and potential oscillations occur. Noticeably, the bivalent nickel species $Ni(OH)_2$, which acts as an electronic mediator, is recovered via (2) and (3). Accompanying the oscillations, periodic oxygen evolution was observed which appeared at the higher

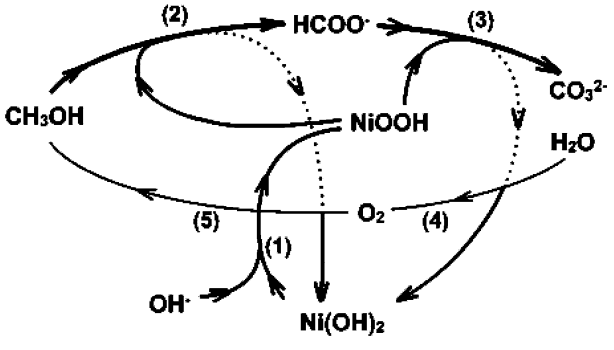

Fig. 8 A mechanistic network diagram for the oscillatory electrocatalytic oxidation of methanol on the NNHF electrode

potential side only and stopped at the lower potential side. Also, oscillations stopped immediately on constant stronger agitation and the potential stabilized at the lower potential side, because no effective depletion of methanol can occur. Clearly, the two opposite electrode processes, i.e. depletion and replenishment of the methanol surface concentration by oxidation under diffusion control and by convection through oxygen evolution, respectively, play key roles in the potential oscillations.

Conclusions

The oscillations of potential for methanol electrocatalytic oxidation on the NNHF electrode in alkaline solution have been studied by in-situ Raman spectroscopy in combination with electrochemical measurements. The film electrode has better electrocatalytic activity for methanol oxidation as a result of a mediated electron-transfer process involving $Ni(OH)_2/NiOOH$ redox pair. Formate and carbonate, respectively, are intermediate and final soluble products from methanol oxidation on this film. Experimental results show that diffusion mass transfer is the rate-determining step for methanol electro-oxidation. Unlike on Pt electrodes, where CO_{ad} formation and removal play the key role, coupling of charge transfer with diffusion and convection mass transfer accounts for the oscillation in methanol electro-oxidation on the NNHF electrode.

Acknowledgements Financial support from Natural Science Foundation of Zhejiang Province of China (202129), and from National Natural Science Foundation of China (20073012), is gratefully acknowledged.

References

1. Mueller E (1923) Z Elektrochem 29:264
2. Mueller E, Hindemith G (1927) Z Elektrochem 33:562
3. Mueller E, Tanaka S (1928) Z Elektrochem 34:256
4. Horanyi G, Inzelt G, Szetey E (1977) J Electroanal Chem 81:395
5. Hudson JL, Tsotsis TT (1994) Chem Eng Sci 49:1493
6. Parsons R, VanderNoot T (1988) J Electroanal Chem 257:9
7. Beden B, Léger JM, Lamy C (1992) Electrocatalytic oxidation of oxygenated aliphatic organic compounds at noble metal electrodes. In: Bockris JO'M, Conway BE, White RE (eds) Modern aspects of electrochemistry, vol 22. Plenum, New York, pp 97–264
8. Jarvi TD, Stuve EM (1998) Fundamental aspects of vacuum and electrocatalytic reactions of methanol and formic acid on platinum surfaces. In: Lipkowski J, Ross PN (eds) Electrocatalysis. Wiley, New York, pp 75–154
9. Iwasita T (2002) Electrochim Acta 47:3663
10. Wasmus S, Kuver A (1999) J Electroanal Chem 461:14
11. Chen YX, Miki A, Ye S, Sakai H, Osawa M (2003) J Am Chem Soc 125:3680
12. Tian ZQ, Ren B, Wu DY (2002) J Phys Chem B 106:9463
13. Weinberg NL, Weinberg HR (1968) Chem Rev 68:449
14. Kaulen J, Schäfer HJ (1982) Tetrahedron 38:3299
15. Hui BS, Huber CO (1982) Anal Chim Acta 134:211
16. Casella IG, Desimoni E, Cataldi TRI (1991) Anal Chim Acta 248:117
17. Luo P, Zhang F, Baldwin RP (1991) Anal Chim Acta 244:169
18. Casella IG, Desimoni E, Salvi AM (1991) Anal Chim Acta 243:61
19. Marioli JM, Luo PF, Kuwana T (1993) Anal Chim Acta 282:571
20. Marioli JM, Kuwana T (1993) Electroanalysis 5:11
21. Fleischmann M, Korinek K, Pletcher D (1971) J Electroanal Chem 31:39
22. Fleischmann M, Korinek K, Pletcher D (1972) J Chem Soc Perkin Trans II 10:1396
23. Robertson PM (1980) J Electroanal Chem 111:97
24. Berchmans S, Gomathi H, Rao GP (1995) J Electroanal Chem 394:267
25. Kowal A, Port SN, Nichols RJ (1997) Catalysis Today 38:483
26. Maximovitch S, Bronoel G (1981) Electrochim Acta 26:1331
27. Archer MD, Corke CC, Harji BH (1987) Electrochim Acta 32:13
28. Amjad M, Pletcher D, Smith C (1977) J Electrochem Soc 124:203
29. Taraszewska J, Roslonek G (1994) J Electroanal Chem 364:209
30. Chen YL, Chou TC (1996) Ind Eng Chem Res 35:2172
31. El-Shafei AA (1999) J Electroanal Chem 471:89
32. Jafarian M, Mahjani MG, Heli H, Gobal F, Heydarpoor M (2003) Electrochem Commun 5:184
33. Vértes G, Horányi G (1974) J Electroanal Chem 52:47
34. Cizewski A (1995) Electroanalysis 7:1132
35. Rostonek G, Taraszewska J (1992) J Electroanal Chem 325:285
36. Huang W, Li ZL, Peng YD, Niu ZJ (2004) Chem Commun 12:1380
37. Li ZL, Ren B, Xiao XM, Zeng Y, Chu X and Tian ZQ (2002) J Phys Chem A 106:6570
38. Granqvist CG (1995) Handbook of inorganic electrochromic materials. Elsevier, Amsterdam.
39. Li ZL, Yu Y, Liao H, Yao SZ (2000) Chem Lett 4:330
40. Li ZL, Ren B, Niu ZJ, Xiao XM, Zeng Y, Tian ZQ (2002) Chin J Chem 20:657
41. Krischer K, Varela H (2003) Oscillations and other dynamic instabilities. In: Vielstich W, Lamm A, Gasteiger HA (eds) Handbook of fuel cells: fundamentals, technology and applications, vol. 2. Wiley, Chichester, pp 679–701
42. Lo YL, Hwang BJ (1998) Langmuir 14:944
43. Weston RE, Jr Ehrenson S, Heinzinger K (1967) J Am Chem Soc 89:481
44. Ito K, Bernstein HJ (1956) Can J Chem 34:170
45. Chang SC, Ho Y, Weaver MJ (1991) J Am Chem Soc 113:9506
46. Bisby RH, Johnson SA, Parker AW, Tavender SM (1998) J Chem Soc Faraday Trans 94(15):2069